

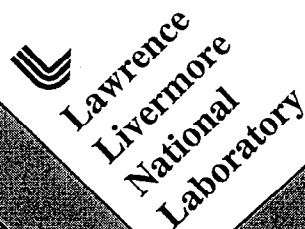
UCRL-JC-127965  
PREPRINT

## Kinetic Modeling of Non-Ideal Explosives with Cheetah

W. Michael Howard  
Laurence E. Fried  
P. Clark Souers

This paper was prepared for submittal to the  
Eleventh International Detonation (1998) Symposium  
Snowmass, CO  
Aug. 31- Sept. 4, 1998

August 6, 1998

The logo of the Lawrence Livermore National Laboratory, featuring a stylized 'U' and 'L' symbol to the left of the text 'Lawrence Livermore National Laboratory' which is arranged in four lines and rotated diagonally.

Lawrence  
Livermore  
National  
Laboratory

This is a preprint of a paper intended for publication in a journal or proceedings. Since changes may be made before publication, this preprint is made available with the understanding that it will not be cited or reproduced without the permission of the author.

#### DISCLAIMER

This document was prepared as an account of work sponsored by an agency of the United States Government. Neither the United States Government nor the University of California nor any of their employees, makes any warranty, express or implied, or assumes any legal liability or responsibility for the accuracy, completeness, or usefulness of any information, apparatus, product, or process disclosed, or represents that its use would not infringe privately owned rights. Reference herein to any specific commercial product, process, or service by trade name, trademark, manufacturer, or otherwise, does not necessarily constitute or imply its endorsement, recommendation, or favoring by the United States Government or the University of California. The views and opinions of authors expressed herein do not necessarily state or reflect those of the United States Government or the University of California, and shall not be used for advertising or product endorsement purposes.

# KINETIC MODELING OF NON-IDEAL EXPLOSIVES WITH CHEETAH

W. Michael Howard, Laurence E. Fried and P. Clark Souers  
Energetic Materials Center  
Lawrence Livermore National Laboratory  
Livermore, CA 94550

We report an implementation of the Wood-Kirkwood kinetic detonation model based on multi-species equations of state and multiple reaction rate laws. Finite rate laws are used for the slowest chemical reactions. Other reactions are given infinite rates and are kept in constant thermodynamic equilibrium. We model a wide range of ideal and non-ideal composite energetic materials. We find that we can replicate experimental detonation velocities to within a few per cent, while obtaining good agreement with estimated reaction zone lengths. The detonation velocity as a function of charge radius is also correctly reproduced.

## INTRODUCTION

The detonation of an energetic material is the result of a complicated interplay between chemistry and hydrodynamics. While the detailed chemical kinetics of detonation in gases have been extensively studied, much less is known regarding chemical kinetic processes governing condensed energetic materials. The primary reason for this is the extreme pressure and temperature immediately behind the detonation wave: pressures of 400 kBar (40 GPa) and temperatures of 4000K are common. The extreme conditions result in very broad spectroscopic features that make the identification of individual chemical species very difficult.

There is a continuing need in the energetic materials field for reliable predictions of detonation velocity and energy delivery. This has traditionally been accomplished through the means of Chapman-Jouget thermodynamic detonation theory. Chapman-Jouget detonation theory assumes that thermodynamic equilibrium of the detonation products is reached instantaneously.

For the purpose of this study we define non-ideal explosives as those with a reaction zone of *one mm* or more. So-call "non-ideal" explosives are often poorly modeled by Chapman-Jouget the theory. These materials have chemical reaction rates that are slow compared to hydrodynamic time scale  $10^{-6}$  s so that the Chapman-Jouget (CJ) assumption of instantaneous thermodynamic equilibrium breaks down. For example, it is found experimentally that the detonation velocity of non-ideal explosives varies sharply from the CJ value and depends strongly on the charge radius.

We are therefore forced to consider the interaction of chemical kinetics with the detonation wave in order to reach an acceptable representation of detonation in non-ideal explosives. Wood and Kirkwood<sup>1</sup> (WK) proposed a two dimensional steady state kinetic detonation theory that solves many of the limitations of ZND theory. WK considered a cylindrical charge of infinite length. They solved the hydrodynamic Euler equations in the steady state limit along the central streamline of the cylinder. Radial expansion was treated as a source term in the 1-D flow along the streamline.

The WK equations have been extensively analyzed by Erpenbeck<sup>2</sup> and co-workers. It is found that the detonation velocity depends on the interplay between chemical kinetics and radial expansion. In the limit of no radial expansion, the ZND plane wave result is obtained. When radial expansion is allowed however, the detonation velocity can vary from the C-J prediction. In the limit of strong radial expansion the detonation wave fails; no velocity is found which satisfies the steady-state equations. Bdzil has generalized WK theory to off-axis flow<sup>3</sup> and Stewart<sup>4</sup> and coworkers have studied the effect of kinetic rates on the decrease of detonation velocity with decreasing size and on curvature of the detonation wave.

In the present paper we implement a model of detonation kinetics based on the identification of individual chemical species. The advantage of the present treatment is that the same equations of state and chemical rate laws can be used on a wide range of explosive mixtures. A mixture equation of state based on thermal, mechanical, and partial chemical equilibrium is used. The mixture model is implemented in the Cheetah thermochemical code<sup>5</sup>. Small molecules that are gases at standard conditions are treated with the

BKW<sup>6</sup> real gas equation of state. Solids are treated with a Murnaghan<sup>7</sup> equation of state. Simple pressure-dependent chemical reaction rates are employed. These rates represent the consumption of the energetic material by the detonation wave. Fast reaction rates (partial chemical equilibrium) are assumed for species other than the initial material.

The Wood-Kirkwood equations are solved numerically to find the steady-state detonation velocity. The radial expansion is derived from measured radii of curvature for the materials studied. We find good agreement with measured detonation velocities *using the same set of equations of state and rate laws for each composite*. Although our treatment of detonation is by no means exact, the ability to model a wide range of phenomena based on simple equations of state and rate laws is encouraging. We find that the inclusion of detonation kinetics yields a significant improvement in the predicted detonation velocity of materials with long estimated reaction zones. More importantly, we are able to reproduce the dependence of the detonation velocity on charge radius for several materials. For materials with short reaction zones, we recover the results of Chapman-Jouget thermochemistry.

## WOOD-KIRKWOOD DETONATION THEORY

WK theory starts with the hydrodynamic Euler equations coupled to chemical kinetics. The theory treats the detonation along the center of the cylinder. The Euler equations are reduced to their steady state form. The result is a set of ordinary differential equations that describe hydrodynamic variables and chemical concentrations along the center of the cylinder.

The notation is as follows: we use cylindrical coordinates in a frame *moving with the shock velocity*  $D$ .  $x$  is the axial coordinate,  $r$  is the radial coordinate and  $u$  is the axial particle velocity in the moving frame (equal to  $D-U$  in the lab frame). The radial velocity is called  $\omega$ . Subscripts denote a spatial derivative.

$$\begin{aligned} u_x &= \psi/\eta \\ \rho_x &= -(\rho/u)(u_x + 2\omega) \\ E_x + p v_x &= 0 \\ \mathbf{F}_x &= \mathbf{R}/u \\ \omega_r &= (D - u(t=0)) / R_c \end{aligned} \quad (1)$$

where  $\mathbf{F}$  is the concentration vector,  $\mathbf{R}$  is the reaction rate vector and  $R_c$  is the radius of curvature.  $\rho$  is the density,  $p$  is the pressure,  $E$  is the specific energy and  $v$  is the specific volume. We take the form of these equations from Fickett and Davis<sup>8</sup> (see Equations 5.28

and 5.37). The expression for  $\omega_r$  is an approximation that is strictly valid only at the initial jump off of the shock.

We define

$$\eta \equiv 1 - u^2/c^2 \quad (2)$$

to be the *sonic parameter*, where  $c$  is the speed of sound. If the sonic parameter  $\eta$  is greater than zero communication with the shock front is possible. If it is less than zero the region cannot communicate with the shock front. Secondly, we will define the *pressure production* term

$$\psi \equiv (\partial P / \partial \mathbf{F})_{v,E} \cdot \mathbf{R} / \rho c^2 - 2\omega_r \quad (3)$$

Chemical reactions that increase the pressure at constant  $v,E$  will increase the value of  $\psi$ . Radial expansion, however, decreases the pressure through the  $\omega_r$  term.

## SOLUTION OF THE WK EQUATIONS

The initial conditions for the WK equations are the energy, density, and composition at the start of the shock front. We specify the initial composition to be the same as the unreacted material. The initial energy and density can be determined by specifying the detonation velocity; finding the intersection of the unreacted shock Hugoniot with the Rayleigh line yields the pressure and density at the shock front. This can be done if the shock velocity is specified. From this point on, the system visits a series of  $(p,v)$  states of different  $P$  with different chemical concentrations. A thermodynamic equilibration at fixed composition then determines the energy at the shock front. Note that the detonation velocity is treated as a *specified quantity* here.

As the equations are integrated, the shockwave structure is determined for positions behind the shock front. In practice, we use the "Lagrangian time" form of the WK equations, where the time variable is related to position by

$$dx = u dt \quad (4)$$

This choice of variables is most natural for the integration of kinetic laws.

The WK equations support a variety of solutions that have been discussed in great detail by Erpenbeck. Let us consider the behavior of the equations as a function of the specified detonation velocity  $D$ . There are three qualitatively different solutions possible. For special

detonation velocities, the solutions pass through the sonic plane, defined by  $\eta = 0$ . Points behind the sonic plane cannot communicate with the shock front. The WK equations are finite when  $\eta = 0$  only if  $\psi$  also passes through zero. Therefore the sonic solutions are defined by the nonlinear equation

$$\psi(t,D) = \eta(t,D) = 0 \quad (5)$$

It is possible to think of this as the kinetic CJ condition. The next possibility is that  $\eta$  never passes through zero. These solutions are *overdriven*; that is the pressure increases with distance behind the shock front. These solutions correspond to a rear piston boundary condition that drives the shock front forward. Finally, if  $\eta = 0$  when  $\psi \neq 0$ , the equations become infinite. This means that a steady state flow cannot occur at the specified detonation velocity  $D$ .

Of all the solutions generated by the WK equations, only the sonic solutions have the pressure tend to zero as  $x$  becomes large. It is these solutions that correspond to steady-state self-propagating flow.

## MIXTURE EQUATION OF STATE MODEL

We now specify the equation of state used to model molecular mixtures. We treat the chemical equilibrium between  $N$  supercritical fluid or gaseous species and  $M$  condensed species. Condensed species  $i$  has  $C_i$  distinct phases. The Helmholtz free energy is a function of the system volume  $V$ , the temperature  $T$ , the molar concentrations of the fluid species  $x$  and the molar concentrations of the condensed species  $X$ . Since the gaseous and condensed species are assumed to be in separate phases, the Helmholtz free energy has the form:

$$A(x, X, V, T) = A^{\text{gas}}(x, V_g, T) + A^{\text{cond}}(X, V_c, T) \quad (6)$$

Here  $V_g$  is the volume of the gaseous phase and  $V_c$  is the volume of the condensed phase, so that  $V_g + V_c = V$ .

We now consider the condensed and gaseous contributions to the Helmholtz free energy separately. The gaseous free energy can be separated into an ideal gas contribution and an "excess" contribution:

$$A^{\text{gas}}(x, V_g, T) = A^{\text{ideal}}(x, V_g, T) + A^{\text{ex}}(x, V_g, T) \quad (7)$$

For the ideal gas portion of the Helmholtz free energy, we use a polyatomic model including electronic, vibrational, and rotational states. Such a model can be conveniently expressed in terms of the heat of formation, standard entropy, and constant pressure heat capacity  $C_p(T)$  of each species. The excess

portion of the free energy comes from a real gas equation of state. In the present paper a BKW equation of state is used. The BKW parameters and covolumes are fitted *only to ideal explosives* and the resulting values are given in Table 1. We call this parameter set BKWC2.

We now turn to the condensed portion of the free energy. The  $i$  th condensed species has  $C_i$  condensed phases, which may possibly coexist in thermodynamic equilibrium. This yields the form:

$$A^{\text{cond}}(X, V_c, T) = \sum_i \sum_j X_{ij} A_{ij}(P, T) \quad (8)$$

with a summation over all species and phases. Here,  $X_{ij}$  is the molar concentration of the  $j$  th phase of species  $i$ .  $A_{ij}(P, T)$  is the molar free energy of the  $j$  th phase of species  $i$ .

TABLE 1. BKWC2 PARAMETERS AND COVOLUMES (CV)

Gas species	CV	Gas species	CV
al	340.0	alo	738.0
c	250.0	c <sub>2</sub> h <sub>4</sub>	211.0
c <sub>2</sub> h <sub>6</sub>	695.9	ccl <sub>2</sub> o	502.2
cf <sub>2</sub> o	811.4	ch <sub>2</sub> f <sub>2</sub>	1318.7
ch <sub>2</sub> o	1455.1	ch <sub>2</sub> o <sub>2</sub>	535.7
ch <sub>3</sub>	382.7	ch <sub>3</sub> oh	990.9
ch <sub>4</sub>	126.0	chf <sub>3</sub>	1152.1
chfo	864.7	cl	234.0
cl <sub>2</sub> op	2300.0	cl <sub>3</sub> p	1890.0
clh	151.3	clk	1810.0
co	340.9	co <sub>2</sub>	522.9
cp	1090.0	f <sub>2</sub>	343.0
h <sub>2</sub>	30.4	h <sub>2</sub> o	226.2
h <sub>2</sub> n	754.2	hf	1214.3
ko	1030.0	n <sub>2</sub>	369.3
no	305.0	no <sub>2</sub>	1964.7
o <sub>2</sub>	305.1	o <sub>2</sub> si	1010.0
osi	653.0	p	271.0
ch <sub>2</sub> f <sub>2</sub>	1318.7	clh	151.3
p <sub>2</sub>	910.0	si	316.0

$\alpha$	0.52080	$\beta$	0.40186
$\theta$	3826.71	$\kappa$	12.31176

The molar free energy  $A_{ij}$  is expressed as a "reference" part at standard pressure, and a part due to pressure:

$$A_{ij}(P, T) = A_{ij}^{\circ}(T) + \Delta A_{ij}(P, T) \quad (9)$$

The reference part is determined through the JANAF compilations of thermochemical data at standard

pressure.  $\Delta A_{ij}$  is determined by the condensed equation of state. We use a modified Murnaghan equation of state as follows:

$$V = V_0 [n \kappa P + \exp\{-\alpha (T - T_0)\}]^{-1/n} \quad (10)$$

$V_0$  is the molar volume when  $P=0$  and  $T=T_0$ .  $\kappa$  is the inverse of the isothermal bulk modulus.  $T_0$  is the temperature of the reference isotherm taken to be 298.15K.  $\alpha$  is the volumetric coefficient of thermal expansion.  $n$  is the derivative  $dB(P,T)/dP$ . We have calibrated the Murnaghan equation of state for the materials used in the present study to shock Hugoniot data<sup>9</sup> and other thermodynamic measurements. These parameters are given in Table 2.

TABLE 2. PARAMETERS FOR THE CONDENSED EQUATIONS OF STATE

Material	$V_0$ cc/mol	$\alpha$ $10^4 K^{-1}$	B GPa	n
HMX	155.47	0.00	10.008	8.50
PETN	177.64	0.00	13.715	5.92
AP	61.133	0.00	12.316	5.59
TNT	137.32	0.00	3.435	9.27
TATB	133.28	0.00	16.290	5.72
NM-LIQUID	52.621	0.00	3.063	5.56
RDX	122.98	0.00	14.923	5.44
VITON	202.25	0.00	12.005	4.99
HTPB	110.75	0.00	2.426	7.96
PARAFFIN	327.52	0.00	8.927	4.88
KEL-F	204.69	0.00	6.286	5.44
CEF	200.35	0.00	5.718	7.00
NC-12.2	161.34	0.00	6.631	7.00
al <sub>2</sub> O <sub>3</sub>	25.720	0.162	303.79	2.50
al	9.948	0.690	78.049	3.80
c-graphite	5.439	0.232	43.731	5.52
c-diamond	3.419	0.024	441.50	4.00
c-liquid	7.065	0.233	11.035	4.00

## APPLICATION TO COMPOSITE ENERGETIC MATERIALS

The detailed chemistry of composite energetic materials is very complicated. Very many chemical steps are involved in the decomposition of most large energetic material molecules into small simple product molecules. In general the composition reactions are not well characterized, especially at elevated temperatures. The situation is made more complicated by the heterogeneous composite nature of most energetic materials. Void collapse and shear dislocations can lead to so-called "hot spots"- regions of enhanced temperature behind the detonation front. These regions play an essential role in high explosive initiation. They preclude describing the energetic material with a single temperature, and complicate the use of even the simplest Arrhenius chemical kinetic schemes.

Most reactive flow models of high explosive initiation overcome these difficulties through the use of pressure-dependent rates. Pressure-dependent rate laws have been shown to be sufficiently flexible to model a variety of initiation and non-ideal detonation phenomena, while maintaining simplicity. The disadvantage of these rate laws is that they do not explicitly treat the high explosive microstructure or the underlying activated chemical reaction rate laws.

We have inferred effective kinetic rates proportional to  $P^2$  for a variety of ideal and non-ideal explosives and their composites. We find that this choice, while simpler than most reactive flow rate laws for high explosive initiation, is adequate to model steady-state detonation over the range of materials and diameters provided here. It has been noted that the detonation velocity size effect is sensitive to particle size. Many of the samples considered here are not fully characterized with regard to particle size, so we do not include dependence of kinetic rate laws on particle size.

We also predict sonic reaction zone widths. The sonic reaction zone width is the length of the zone behind the detonation wave for which the local velocity of sound is equal to or greater than the detonation velocity. This zone is where chemical reactions contribute to the detonation wave. Beyond this zone, chemical reactions do not contribute the detonation wave.

For the purposes of this study, we model the kinetic processes of the high explosives as being a single decomposition reaction into primary product constituents. The reaction products that we have assumed for the various high explosives, binders and metal reactions are listed in Table 3. However, because we assume that all of the products are in thermochemical equilibrium, the results are independent of the assumed decomposition pathway. This would not be the case if reversible reactions were important.

TABLE 3. EFFECTIVE CHEMICAL REACTIONS CONTROLLED BY KINETICS.

Reactant	Products	R $\mu s^{-1} GPa^{-2}$
al, O <sub>2</sub>	al <sub>2</sub> O <sub>3</sub>	0.0075
AP	n <sub>2</sub> , h <sub>2</sub> O, O <sub>2</sub> and hcl	0.0075
CEF	c <sub>2</sub> h <sub>4</sub> , O <sub>2</sub> , cl and p	0.01
HMX	co <sub>2</sub> , h <sub>2</sub> and n <sub>2</sub>	0.2
HTPB	c, ch <sub>4</sub> and h <sub>2</sub> O	0.001
KEL-F	c, chf <sub>3</sub> , f <sub>2</sub> and cl	0.01
NC-12.2	co <sub>2</sub> , h <sub>2</sub> O and n <sub>2</sub>	0.01
NM	co <sub>2</sub> , n <sub>2</sub> , h <sub>2</sub> O and c	1.0

PARAFFIN	c and $ch_4$	0.01
PETN	$co_2$ , $h_2o$ , $n_2$ and c	0.50
RDX	$co_2$ , $h_2o$ , $n_2$ , $o_2$ and c	0.20
TATB	$n_2$ , $h_2o$ , $co_2$ and c	0.06
TNT	c, $co_2$ , $h_2o$ and $n_2$	0.10
VITON	c, $ch_3f$ , $ch_4$ and $f_2$	0.01

We assume that the kinetic rates are defined by the following equation:

$$d\lambda/dt = (1 - \lambda)RP^2 \quad (11)$$

where P is the pressure, R is the rate constant (see Table 3) and  $\lambda$  represents the amount of unburned reactant normalized to vary between 0 (all unburned) and 1 (all burned). In our kinetics scheme the concentrations of reactants are assumed to be controlled by the kinetic rate, while all of the products are assumed to be in thermochemical equilibrium.

For non-ideal explosives, the effects of equations of state are strongly coupled to the effects of kinetics and hydrodynamics. For the equations of state, the usual process is to fit the covolumes of the product gases to experimental detonation velocities of ideal and non-ideal explosives. For this study we have used a BKW equation of state for product gases *with parameters fit only to ideal explosives*. The modified Murnaghan EOS of Eq. 10 was fit to shock Hugoniot data for individual product species.

## RESULTS

The explosives mixtures studied here are composed of HMX, NM, RDX, PETN, TATB, TNT and AP, along with a variety of binders. We also model Al combustion in composites. The composites and explosives that we consider are given in Table 4. In modeling these composites, we assume that each component material burns at a rate, which is independent of the other components in the composite. We find that this simple approximation is adequate to describe the detonation velocity of the materials studied here. It should be noted that the approximation may fail for certain materials, most notably binary fuel/oxidizer mixtures, where the presence of one component dramatically accelerates the reaction of the other. Most of the composites contain a single high explosive and a binder. The composites with three or more components include IRX-3A, IRX-4 and PBXN-111. Each rate law was based on calculating the detonation velocity of several materials. The rate laws were adjusted to give the best fit to the experimental detonation velocity and where available the estimated reaction zone. The data for

Table 4, as well as the experimental detonation velocities in Table 5, are taken from Ref. 10.

TABLE 4. DENSITY  $\rho$ , CHARGE RADIUS  $R_o$ , AND RADIUS OF CURVATURE  $R_c$  OF COMPOSITE ENERGETIC MATERIALS STUDIED HERE.

Composite	$\rho$ (g/cc)	$R_o$ (mm)	$R_c$ (mm)
COMP-B	1.670	25.43	201.61
EDC-35(1)	1.904	5.00	21.74
EDC-35(2)	1.904	25.40	199.20
IRX-1	1.430	25.0	206.61
IRX-3A	1.580	25.0	177.30
IRX-4	1.500	25.0	130.55
LX-04	1.863	12.70	228.31
LX-17	1.907	25.40	206.61
NM(1)	1.118	6.35	114.68
NM(2)	1.124	9.57	79.11
NM(3)	1.124	13.78	279.33
NM(4)	1.124	18.42	526.32
NM(5)	1.118	25.40	739.64
OCTOL	1.809	12.70	223.21
PBX-9404	1.840	12.70	495.05
PBX-9502(1)	1.895	5.00	29.76
PBX-9502(2)	1.895	5.00	30.49
PBX-9502(3)	1.895	6.00	39.06
PBX-9502(4)	1.895	9.00	66.58
PBX-9502(5)	1.895	25.0	246.31
PBX-9502(6)	1.895	25.0	226.24
PBXN-110	1.68	24.95	245.10
PBXN-111(1)	1.790	12.60	51.90
PBXN-111(2)	1.790	18.95	107.40
PBXN-111(3)	1.790	23.49	143.30
PBXN-111(4)	1.790	50.00	479.80
PENTOLITE	1.560	25.40	56.31
TATB	1.808	12.70	132.98
TNT	1.621	12.70	274.73

A summary of our results is presented in Table 5. There are notable deficiencies in the C-J detonation velocity calculations when compared to experiment. In Figure 1 we compare detonation velocities calculated with C-J theory using the BKWC2 parameter set to experimental values. There is good agreement between theory and experiment for the compounds with experimental detonation velocities greater than 8 km/s. These materials are predominantly high explosive with less than 10% binder by weight. The deviation between C-J theory and experiment is quite substantial for experimental detonation velocities less than 8 km/s. These materials are multi-component mixtures containing AP and Al. Generally there is more than 10% of the binder material present by weight.

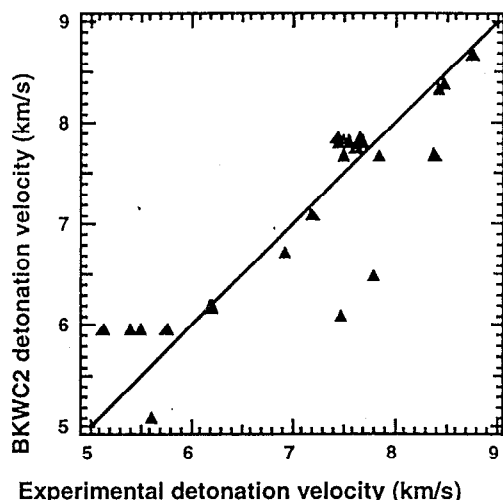


FIGURE 1. DETONATION VELOCITIES (IN KM/S) AS CALCULATED WITH C-J THEORY AND THE BKWC2 EQUATION OF STATE PARAMETER SET.

TABLE 5. CALCULATED DETONATION VELOCITIES IN KM/S WITH BKWC2 (W2), BKWS (WS) AND WK, EXPERIMENTAL DETONATION VELOCITIES (EXP) AND CALCULATED REACTION ZONES (RZ).

COMPOSITE	W2	WS	EXP	WK	RZ mm
COMP-B	7.67	8.02	7.86	7.65	0.40
EDC-35(1)	7.85	8.07	7.44	7.44	0.46
EDC-35(2)	7.85	8.07	7.67	7.74	0.68
IRX-1	6.10	7.11	7.49	7.10	0.59
IRX-3A	6.48	7.36	7.79	7.30	0.41
IRX-4	5.10	6.67	5.62	4.98	2.02
LX-04	8.38	8.40	8.48	8.28	0.49
LX-17	7.75	7.97	7.63	7.66	0.80
NM(1)	6.16	6.58	6.20	6.12	0.22
NM(2)	6.18	6.60	6.21	6.13	0.20
NM(3)	6.18	6.60	6.23	6.15	0.24
NM(4)	6.18	6.60	6.23	6.15	0.24
NM(5)	6.16	6.58	6.21	6.14	0.27
OCTOL	8.33	8.68	8.42	8.29	0.27
PBX-9404	8.67	9.00	8.75	8.59	1.42
PBX-9502(1)	7.81	8.04	7.46	7.49	0.49
PBX-9502(2)	7.81	8.04	7.46	7.49	0.49
PBX-9502(3)	7.81	8.04	7.50	7.55	0.52
PBX-9502(4)	7.81	8.04	7.55	7.63	0.58
PBX-9502(5)	7.81	8.04	7.68	7.73	0.77
PBX-9502(6)	7.81	8.04	7.67	7.73	0.78
PBXN-110	7.68	8.31	8.39	8.37	0.25
PBXN-111(1)	5.97	7.45	5.13	4.78	1.52
PBXN-111(2)	5.97	7.45	5.41	5.44	7.39
PBXN-111(3)	5.97	7.45	5.51	5.62	7.94
PBXN-111(4)	5.97	7.45	5.75	5.97	8.65

PENTOLITE	7.09	7.37	7.19	6.95	0.48
TATB	7.68	7.92	7.50	7.56	0.72
TNT	6.72	7.12	6.92	6.68	0.89

We also performed C-J calculations with the larger BKWS<sup>11</sup> product set. The results are given in Table 5 and Fig. 2. The BKWS predictions for the detonation velocity are accurate when the experimental detonation velocity is more than 7 km/s. Below this point, substantial deviations between theory and experiment remain. The BKWS product set predicts velocities more accurately than BKWC in the range of 7-8 km/s. This may be due to the calibration of BKWS, which was performed on a database of ideal and non-ideal explosives, while BKWC2 was calibrated solely to ideal explosives.

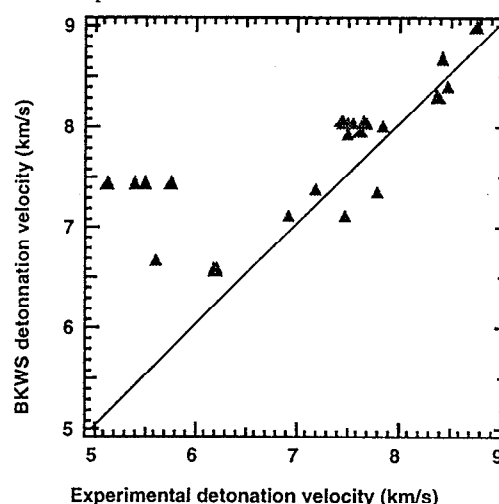


FIGURE 2. DETONATION VELOCITIES (IN KM/S) AS CALCULATED WITH C-J THEORY AND THE BKWS EQUATION OF STATE PARAMETER SET

In Figure 3 we plot detonation velocities obtained with WK detonation theory and the reactions given in Table 3. The kinetic calculations are nearly as accurate at detonation velocities around 5 km/s as they are at 8 km/s. Although the calculations are not exact, all the large deviations from experiment have been eliminated.

Some of the non-ideal explosives that we study have significant amounts of hydrol-terminated poly butiene (HTPB). These non-ideal composites include IRX1, IRX-3A, IRX4, PBXN-110 and PBXN-111. Table 5 gives the compositions of these composites. We find it interesting that the products of this binder are hydrocarbons such as  $CH_4$  and  $C_2H_6$ . For these cases the calculated detonation velocities are sensitive to the equations of state for these hydrocarbons. Unfortunately, there is only shock data for methane and not ethene or other hydrocarbons.



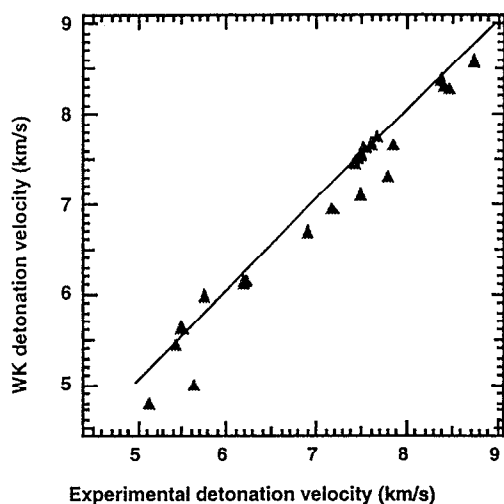


FIGURE 3. DETONATION VELOCITIES (IN KM/S) AS CALCULATED WITH WK THEORY AND THE BKWC2 EQUATION OF STATE PARAMETER SET.

TABLE 6. NON-IDEAL COMPOSITES

Composite	Composition by weight
PBXN-110	HMX, 88%, HTPB, 12%
PBXN-111	RDX, 20%, AP, 43%, AL, 25%, HTPB, 12%
IRX1	HMX, 70.1%, HTPB, 29.9%
IRX-3A	HMX, 69.8%, AL, 10%, HTPB, 20.2%
IRX4	HMX, 30%, AP, 24%, AL, 16%, HTPB, 30%

Figure 4 shows our results for PBXN-111. The solid circles are the experimental detonation velocity as a function of radius from Forbes and Lemar<sup>12</sup>, while the open circles are our calculated values. Our calculated values reproduce the experimental values reasonably well, while using generic kinetic rates given in Table 3. The shape of the curve, however, is sensitive to the rates chosen for AP and Al. In addition, for PBXN-111 we find multi-valued solutions<sup>4</sup> for the detonation velocity. In such a case we take the largest value.

At this point it is still difficult to differentiate some kinetic effects from equation of state effects. Take for example the case of HTPB. The three composites that we model with at least three components (see Table 6) contain HTPB, as well as Al and also ammonium perchlorate (except IRX-3A). It is interesting to notice that all of the explosive composites with the HTPB binder exhibit significant non-ideal behavior. In particular, we find that we must model HTPB to have a very slow kinetic rate (less than  $0.1 \mu s^{-1}$ ). Kinetic rates for HTPB faster than  $0.1 \mu s^{-1}$  have a significant

effect on the calculated detonation velocity for these composites. Other explosives with significant amounts of binder also exhibit significant non-ideal effects. In addition, TATB with only small amounts of binder (PBX-9502) also exhibits non-ideal behavior. The largest non-ideal effects in the detonation velocity exist for PBX-9502, PBXN-110, IRX-1, IRX-3A, PBXN-111 and IRX-4. For the most part these composites contain large amount of binder and/or metal. For all of the composites listed, there are radius of curvature measurements<sup>10</sup>.

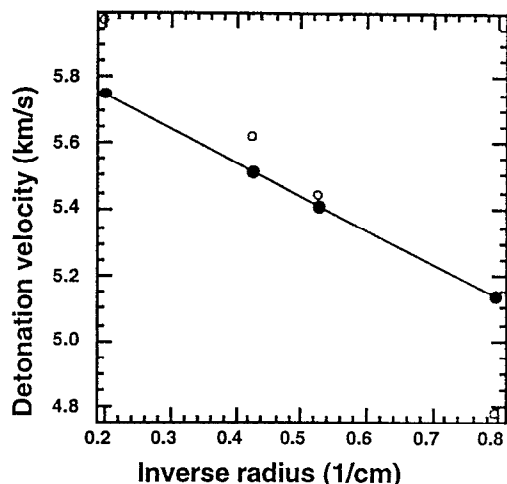


FIGURE 4. WK THEORY PREDICTS THE DETONATION VELOCITY AS A FUNCTION OF SIZE FOR PBXN-111.

Almost half of the composites (8 out of 16) listed in Table 4 exhibit significant non-ideal behavior. That is, the experimental detonation velocity is significantly different than the calculated C-J theory detonation velocity. The composites exhibiting significant non-ideal behavior include EDC-35, PBX-9502, PBXN-110, TATB, IRX-1, IRX-3A, PBXN-111 and IRX-4. Seven of these composites contain RDX or HMX, which should have similar kinetic properties. Among these seven composites, there is a correlation between the amount of binder and the percent deviation of the experimental al detonation velocity from that predicted by the C-J theory. The one exception to this correlation is IRX-4, which is a multi-component composite containing 24% AP and 16% Al. We have no explanation for this except to note that a multi-component composite may have complex interactions between the kinetic rates of its constituents.

It is also interesting to calculate the case for which there is data for the detonation velocity and radius of curvature for composites as a function of charge radius. There are three composite explosives for which we have data. These are PBXN-111, PBX-9502 and

NITROMETHANE (NM). This is interesting because PBXN-111, and to a less extent PBX-9502 (with is 95% TATB by weight), exhibits significant non-ideal behavior. For PBXN-111 and PBX-9502, our calculated detonation velocities decrease faster with decreasing radius than the experimental detonation velocities.

Kennedy and Jones<sup>13</sup> have previously studied the non-ideal behavior of PBXN-111. Experiments with PBXN-111 have been performed from a charge radius of 50 cm., down to the failure radius which is less than 9.5 cm. Previous estimates of the equilibrium C-J detonation velocity of PBXN-111 by Kennedy and Jones range from 6.75 to 8.00 km/s. Our estimate of the equilibrium C-J detonation velocity of PBXN-111 is 5.97 km/s. A significant difference between our calculations and previous ones, is that with our carbon equation of state we predict all of the carbon is in the gas state at the C-J point, while Kennedy and Jones predict a significant amount of diamond is produced at that state.

In conclusion we have developed a kinetic model for thermochemical detonations based on Wood-Kirkwood theory and the thermochemical Cheetah code. We find that with a simple model for kinetic processes we are able to model many of the features of non-ideal explosives such as their detonation velocities and their sonic reaction zone widths. In the future, we plan to extend our kinetic modeling study to include temperature and pressure dependent rate laws. In this way we can extend our model to more physically based rate laws and study more complex non-ideal detonation behavior such as shock initiation, hot spot formation and failure processes.

## ACKNOWLEDGMENTS

This work was performed under the auspices of the U. S. Department of Energy by the Lawrence Livermore National Laboratory under contract No.-W-7405-48. This work was supported by the Accelerated Strategic Initiative (ASCI) at Lawrence Livermore National Laboratory. We especially thank C. Souers for compilation all of the experimental data, which made this study possible.

## REFERENCES

1. Wood, W. W. and Kirkwood, J. G., "Diameter Effect in Condensed Explosives", *J. Chem. Phys.*, **22**, 1954, pp. 1920-1924.
2. Erpenbeck, J. J., "The Stability of Idealized One Dimensional Detonations", *Phys. Fluids*, **7**, 1964, pp. 684-696.
3. Bdzil, J. B., "Steady-state Two-dimensional Detonation", *J. Fluid. Mech.*, **108**, 1981, pp. 195-206.
4. Stewart, D. S. and Yao, J., "The Normal Detonation Shock Velocity Curvature Relationships for Materials with Non Ideal Equation of State and Multiple Turning Points", *Combustion and Flame*, **113**, 1998, pp. 224-235.
5. Fried, L. E., Howard, W. M. and Souers, P. C., "CHEETAH 2.0 User's Manual", Lawrence Livermore National Laboratory Report UCRL-MA-117541 Rev. 5, 1998.
6. Fried, L. E. and Souers, P. C., "BKWC: AN Empirical BKW Parameterization Based on Cylinder Test Data", *Propellants, Explosives, Pyrotechnics*, **21**, 1996, pp. 215-223.
7. Murnaghan, F. D., *Proc. Natl. Acad. Sci. (USA)*, **30**, 1944, pp. 244-247.
8. Fickett, W. and Davis, W. C., "Detonation", University of California Press, Berkeley, 1979, Chapter 5.
9. Marsh, S. P., "LASL Shock Hugoniot Data", University of California Press, Berkeley, 1980.; see also, Dobratz, B. M. and Crawford, P. C., "LLNL Explosives Handbook Properties of Chemical Explosives and Explosive Simulants", report UCRL-52997 change 2, January 31, 1985.
10. Souers, P. C., "A Library of Prompt Detonation Reaction Zone Data", Lawrence Livermore National Laboratory Report, UCRL-ID-130055, Rev. 1, June, 1998.
11. Hobbs, M. L. and Baer, M. R. , "Calibrating the BKW-EOS with a Large Product Species Data Base and Measured C-J Properties", *Proceedings Tenth International Detonation Symposium*, Boston, MA, July 12-16, 1993, pp. 409-418, 1995.
12. Forbes, J. W. and Lemar, E. R., "Detonation wave velocity and curvature of PBXN-111 as a function of size and confinement", submitted to *J. Appl. Phys.*, 1998.
13. Kennedy, D. L. and Jones, D. A., "Modeling Shock Initiation and Detonation in the Non-ideal Explosive PBXW-115", *Proceeding of the 10th International Detonation Symposium*, Boston Massachusetts, July-12-16, 1993, pp. 665-674, 1995.